Sonochemical hydrogenation of metallic microparticles

Sonochemical hydrogenation of metallic microparticles

A. Troia*, E.S. Olivetti, L. Martino, V. Basso

Istituto Nazionale di Ricerca Metrologica, INRIM, Strada delle Cacce 91, 10135 Torino, Italy

** corresponding author: a.troia@inrim.it*

Abstract

We report the sonochemical synthesis of hydrogenated metallic microparticles through room-temperature ultrasonic irradiation of aqueous metallic slurries. The role of saturating gases and of reduction-oxidation mechanism on promoting the hydride formation is investigated. The method is then applied to study the synthesis of different metallic hydrides (Mn, Ti) and the hydrogenation of $La(Fe,Mn,Si)_{13}$, an intermetallic compound with magnetocaloric properties used in magnetic refrigeration applications. The samples were characterized by X-ray diffraction to identify the presence of hydrogenated phases, by differential scanning calorimetry to evaluate hydrogen release and temperature stability of the hydrides and by electron microscopy to identify morphological modifications induced by acoustic cavitation. The hydrogenation of metallic microparticles and intermetallic compounds is reported for the first time by means of this experimental technique which could represent a new tool for fast and cheap hydrogenation of materials for different technological applications, such as hydrogen storage and magnetic refrigeration.

1. Introduction

Hydrogenation of metals and intermetallics is of great interest because of the variety of applications of metal hydrides, like hydrogen storage systems for fuel cells, nickel metal hydrides batteries, intermetallic compounds for magnetic refrigeration, in catalysis and metallurgy fields, and in high temperature superconductors [1], [2], [3], [4], [5]. The ability of absorbing hydrogen is common to all metals, although the metals differ greatly in how much hydrogen is absorbed and the hydrides formation is ruled by several parameters of the host metal. Crystal structure type, cell size and the enthalpy of hydride formation are some of the parameters that play a fundamental role. Cubic systems, both face-centered (fcc) or body-centered (bcc), are reported to be more suitable for formation of pure metal hydrides with respect to hexagonal closed packed (hcp) metallic structures [6], [7], [8]. Many pressure-composition-temperature diagrams report the operating temperature and pressure conditions in which the hydride formation is thermodynamically favored for each metal or intermetallic compound, however, from the point of view of applications kinetics of the H_2 absorption/desorption process is also important especially for hydrogen storage applications. In this context intermetallics are very attractive since they can form hydride phases almost spontaneously. The high density of the stored hydrogen, as well as safety aspects, are the main reasons for the rapid growth of applied research in this field over the last ten years [9], focused also on thermodynamics aspects of the metal-hydrogen systems [10], and exploring the synthesis of new materials like nanoporous particles or thin films to improve hydrogen sorption properties [11]. The methods usually employed to obtain metallic hydrides involve high pressures (1–100 MPa) and high temperatures, (300–1000 K), up to the extreme conditions (pressures > 200 GPa and

temperature > 1000 K) of the laser-heated diamond anvil cell technique. Other methods as electrochemical or solid state reactions [12] have been used, however, to our knowledge, only one paper reports the use of high intensity ultrasounds to perform the synthesis of a metallic hydride from an aqueous salt solution [13].

Generation of high intensity ultrasounds in a liquid causes the phenomenon of acoustic cavitation, that is the formation, growth and violent collapse of bubbles that reach local high temperatures (up to 5000 K), high pressure (several hundred bars) and extreme cooling rates (10^9 K/s), together with the formation of reactive radical species, which depend on the composition of the sonicated liquid and of the dissolved gases [14]. When bubbles collapse near a solid surface, a shape distortion of bubbles, with formation of high speed liquid-jets, occurs. This phenomenon is the main origin of the mechanical effects which bring to erosion, fragmentation of solid particles or solid surfaces and that is the acting mechanisms for ultrasonic cleaning. Thus, cavitating bubbles act as a sort of micro-reactor creating extreme physical and chemical conditions within the bubbles and at the bubble/solution interface despite the bulk solution remains at room temperature. Chemical applications of this technology, known as sonochemistry, have been used over the last twenty years for synthesis of materials with unique properties, to accelerate the reaction rate of common processes, to develop new synthesis routes in organic chemistry and for pollutant degradation in environmental remediation [15]. Applications of sonochemistry in materials science relies both on physical and chemical effects, however most of the papers devoted to the synthesis of nanostructured materials focuses more on exploiting the acoustic cavitation effects in homogeneous conditions i.e. with metal ions dissolved in solution. On the contrary few works have been reported on the investigation of the chemical effects of sonication on dispersed metallic particles (i.e in heterogeneous conditions). Most of the studies on the influence of ultrasound on metal surfaces and particles have been focused on surface erosion, particles size reduction, agglomeration [16], [17], [18], [19] or efficient dispersion, without a careful analysis of the ultrasounds effects and chemical modifications on the inner structure and composition of the treated particles. Because of the lack of a quantitative understanding of the effects of the cavitating bubbles on solid particles, is difficult to disentangle the mechanical and chemical effects. The liquid jets impinging on the surface of particles and the chemical modifications due to radical species arising from collapsing bubbles, act as synergistic mechanisms that chemically and physically modify the surfaces of the particles. In the last five years some works on the application of high intensity ultrasounds as efficient tool for top-down nanostructuring of multiphase metal systems and metallic particles have been reported [20], [21], [22]. Recent papers by E. Skorb et al. have shown the possibility to conduct ultrasound-assisted modification of metal particles, demonstrating that interfacial reduction-oxidation reactions and temperature-driven solid state phase transformations affect the surface composition and morphology of metals and alloys, respectively. Physical and chemical properties of sonicated medium, as well as metal particle reactivity, strongly affect the structuring pathways and morphology. This technique has been recently used to induce sintering process on metallic alloys microparticles [23], [24], to study the amorphization and the oxidation processes of crystalline silicon surface treated with ultrasound [25], [26] and their effects on chemical and physical modifications of silicon q-dots [27] and finally to obtain alkaline-earth metal hydride with the formation of mesoporous metallic sponges [28]. Here we report the sonochemical hydrogenation of different metallic microparticles that are commonly prepared by very high pressure and high temperature processes. According to the literature [6], [7], [8], metals with bcc and fcc structure can easily form interstitial hydrides because of the bigger empty space within the unit cell and hydrides

of 3d block elements are some of the most thermodynamically favored and stable. For these reasons our experiments were focused on metallic particles of Manganese and Titanium, which are known to give stable hydrides at ambient temperature conditions, in order to investigate the role of different atomic cell structure. Additionally, in order to test this technique on technologically relevant materials, we investigated the hydrogenation of an intermetallic compound studied for magnetic refrigeration applications, namely $La(Fe,Si,Mn)_{13}$, whose magnetic properties are strictly dependent on the hydrogen content. Finally, preliminary tests have been carried out on $LaNi_5$ as well, an intermetallic compound of great interest in hydrogen storage applications. The results obtained point out that the sonochemical technique can be seen as a cheap and fast tool for hydrogenation of metal microparticles and of intermetallic compounds.

2. Materials and methods

2.1. Ultrasonic treatment of metallic slurries

High intensity ultrasonic treatments have been performed by using a 20 kHz sonotrode (Bandelin HD 2200) equipped with Titanium probes (13 or 19 mm of diameter). Aqueous suspensions of 1.6 wt% of metallic microparticles and intermetallic alloys were exposed to pulsed ultrasounds (duty cycle 50%) with the sonotrode operating at 50% of the maximum power, for 90 and 180 min, in a 50 ml or 100 ml glass vessel reactor. For all the treatments performed the temperature of the solution did not exceed 30 °C, by means of the cooling provided by an ice bath or by a cooling water jacket (see Fig. 1). Pulsed treatment was chosen to prevent the erosion of the probe tip and to avoid excessive heating of the solution. According to calorimetric power measurements [29] the power employed in our experiments corresponds to *10 W.* The role of the saturating gas has been investigated using air-saturated solutions and hydrogen-saturated solutions produced by adding Sodium borohydride before the sonication treatment ($NaBH_4$: metal particles weight ratio was 2:1 or 4:1). To avoid the oxidation of metallic particles, in some experiments the effect of a coating polymer like polyvinyl alcohol (PVA, M_w 89000–98000 Da) has been also investigated. Metal microparticles of Mn,Ti and a $La(Fe,Si,Mn)_{13}$ magnetic compound have been used for these experiments. All the samples were centrifuged after treatment and let dry overnight before characterization.

2.2. Materials characterization

The sample phase composition of the metallic powders was investigated by means of X-ray diffraction (XRD) in Bragg-Brentano geometry, with Cu Kα radiation, both in the as-received state and after sonochemical treatments. Lattice parameters, a_0, have been extrapolated from a linear fit of the a_{hkl} vs $\cos\theta\cot g\theta$ plot of all the available experimental reflections. Morphology of the powders has been studied by means of field-emission scanning electron microscopy (SEM). The samples phase transformations and the release of hydrogen upon heating was monitored by power-compensation differential scanning calorimetry (DSC) with a heating rate of 10 K/min. On each sample two heating and cooling scans under the same temperature program were performed to evaluate the reversibility of the processes. The DSC curves displayed below were obtained from the

subtraction of the second heating run from the first one in order to get rid of the baseline signal of the DSC cell.

3. Results and discussion

3.1. Ultrasonic treatment of Mn microparticles

Manganese is a quite active metal and, according to its Pourbaix diagram, it is never immune in contact with water, being capable to react with it either oxidizing to Mn^{2+} ion or forming passivating insoluble species such as $Mn(OH)_2$ or Mn oxides of different oxidation state, depending on pH and electrode potential [30]. The stable allotrope of Manganese at atmospheric pressure and room temperature is α-Mn, with a complex cubic cell containing 58 atoms, stable up to 710 °C. However, at higher temperatures Mn can exist in other allotropic forms, namely β-Mn, γ-Mn and δ-Mn, all with cubic lattices of different symmetry. Under hydrogen pressure and at high temperatures Mn is able to form four different hydride phases: two 'low pressure' hydrides, namely α-MnH_x and β-MnH_x (with $x \leq 0.1$), are solid solutions of hydrogen in α-Mn and β-Mn, respectively, stable up to $p(H_2) < 0.8$ GPa; these are transformed into 'high pressure' hydrides: ε-MnH_x with a hcp cell ($x \geq 0.65$) at lower temperatures, and γ-MnH_x ($0 < x < 0.5$) with fcc structure, at higher temperatures [8], [31]. In all hydrides H atoms partially occupy octahedral interstitial positions. To test the chemical effects of ultrasonic treatment on metallic manganese we have studied two different conditions, in order to assess the influence of the dissolved gas on hydride formation, namely: the sonochemical treatment in deionized water and the sonochemical treatment in presence of a hydrogen-releasing agent ($NaBH_4$), dissolved in water solution. A control experiment with Mn powder immersed in deionized water for 90 min and for 30 days, without any reactant and without ultrasonic irradiation has been carried out as well. In addition, the effect of PVA as coating polymer has been also investigated. Table 1 summarizes the different experimental conditions used and the produced samples, along with their ID, used for the sake of brevity in the rest of the discussion.

Table 1. Summary of experimental conditions tested during the sonochemical experiments on Mn powders and qualitative phase composition of the resulting samples. The lattice parameter of the cubic Mn(H) phase is reported together with the standard error of the linear fit performed to calculate it.

Condition	Treatment	Sample ID	Phases detected
Starting material	none	Pristine Mn powder	α-Mn, $a_0 = 8.9197 \pm 0.0007$ Å Mn_3O_4(traces)
'Natural' oxidation in deionized water	Suspension in water 90 min no coating	NAT-short	α-MnH_x cubic, $a_0 = 8.930 \pm 0.001$ Å Mn_3O_4 MnOOH (traces)
	Suspension in water 30 days no coating	NAT-long	α-MnH_x cubic, $a_0 = 8.952 \pm 0.002$ Å ε-$MnH_{0.85}$ hexagonal

Condition	Treatment	Sample ID	Phases detected
Sonochemical treatment in deionized water	US irradiation 90 min no coating	US-water	Mn_3O_4 α-MnH_x cubic, $a_0 = 8.958 \pm 0.002$ Å ε-$MnH_{0.85}$ hexagonal
	US irradiation 180 min PVA coating	US-PVA	Mn_3O_4 α-MnH_x cubic, $a_0 = 8.951 \pm 0.002$ Å ε-$MnH_{0.85}$ hexagonal
Sonochemical treatment in H_2-rich solution	US irradiation 90 min $NaBH_4$ solution (weight ratio $NaBH_4$:Mn = 2:1) no coating	US-H2 2:1	Mn_3O_4(traces) α-MnH_x cubic, $a_0 = 8.944 \pm 0.002$ Å ε-$MnH_{0.85}$ hexagonal MnO_2
	US irradiation 180 min $NaBH_4$ solution (weight ratio $NaBH_4$:Mn = 4:1) no coating	US-H2 4:1	Mn_3O_4 (traces) $Mn(OH)_2$ (traces) α-MnH_x cubic, $a_0 = 8.959 \pm 0.002$ Å ε-$MnH_{0.85}$ hexagonal MnO (traces)

A first series of experiments involved the sonication of aqueous suspension of Mn microparticles, and their results were compared to the ‘natural oxidation’ in water. Fig. 2 displays the XRD patterns of selected samples treated in deionized water: as one can see from Fig. 2A the Mn peaks of the NAT-short sample (see the details in Table 1) are slightly shifted towards lower angles, indicating a cell expansion with respect to the pristine Mn powder. A short treatment in deionized water (sample ID: ‘NAT-short’) is indeed sufficient to produce a slight oxidation of the Mn powder, and, as a result of availability of hydrogen gas produced through the redox reaction, also a detectable change in Mn lattice parameter (see table I) due to interstitial hydrogen incorporation into the cubic metal cell. The process can be described by the following reaction:

$$4Mn + 4H_2O \rightarrow Mn_3O_4 + MnH_x + (4-x)H_2 \quad (1)$$

In the ‘NAT-long’ sample, kept in water for 1 month, the oxidation proceeded to a greater extent, giving rise to: i) a higher fraction of Mn_3O_4 (hausmannite); ii) a much greater increase of the cubic α-MnH_x lattice parameter and iii) the appearance of the hexagonal hydride, with stoichiometry $MnH_{0.85}$. The XRD patterns in Fig. 2A can be compared with the ones in Fig. 2B, where the Mn powders suspended in water were irradiated with high intensity ultrasounds for 90 min, with and without the addition of the coating polymer PVA: in the uncoated sample (ID: ‘US-water’) three phases are present: the cubic ‘low-pressure’ hydride, α-MnH_x, the hexagonal ‘high-pressure’

hydrideε-$MnH_{0.85}$, and Mn_3O_4. The calculated lattice parameter of the cubic hydride is much larger (8.958 Å) than the one of the corresponding naturally oxidized sample (8.930 Å), indicating a higher degree of hydrogen incorporation into the metal lattice. Thus, during ultrasonic irradiation both oxidation and hydrogenation processes are greatly enhanced, indicating an acceleration of the reaction (1) induced by ultrasounds.

Since in these conditions a strong oxidation of the metallic particles occurs, the same treatment was performed in an aqueous suspension containing 0.5% of polyvinyl alcohol: as expected, the sample treated in presence of PVA has a lower content of Manganese Oxide because of the capping action of PVA which prevents particles oxidation, while both Mn hydrides are again formed. Since the partial oxidation of the sample is commonly an unwanted effect, we decided to treat our samples in hydrogen-rich solutions in order to increase the amount of hydrogen available for reacting with metallic particles and to prevent the oxidation effect. For this purpose aqueous solutions of $NaBH_4$ have been employed to suspend the metallic microparticles. Sodium borohydride is a well known reducing agent in aqueous solutions and its hydrolysis reaction can be exploited for the generation of hydrogen in situ [32], according to the reaction:

$$NaBH_4 + 2H_2O \rightarrow Na^+ + BO_2^- + 4H_2 \quad (2)$$

The metaborate ion (BO_2^-) is strongly basic so, hydrogen evolution is accompanied by an increase in pH of the solution due to its hydrolysis reaction, which, in turn, causes a decrease of the rate of reaction (2).

In this case (see Fig. 3) the formation of both cubic and hexagonal Mn hydrides is attained without significant oxidation. The sample treated in solution with higher $NaBH_4$:Mn weight ratio (US-H2 4:1) shows a higher degree of hydrogenation of the cubic α-MnH_x phase (a_0 = 8.959 Å vs 8.944 Å) and a higher phase fraction of the hexagonal $MnH_{0.85}$ phase, with respect to sample US-H2 2:1. Small intensity peaks of different Mn oxides and hydroxide were also observed.

Fig. 4 displays the SEM images of selected Mn samples, namely: the pristine powder (A), the US-water sample (B), the US-PVA sample (C) and the US-H2 4:1 sample (D). From their comparison it is evident that:i) ultrasonic irradiation produces erosion of the particles edges, which appear rounded in all the treated samples; ii) the surface morphology of the PVA-coated sample is quite different from the uncoated ones, the latter being characterized by tiny crystals (100–200 nm in diameter) surrounding the particles, presumably composed of Mn-oxide species, also detected in the corresponding XRD patterns. The particles of the PVA-coated sample are instead quite smooth and free from nanocrystals growth, in agreement with the results of XRD analysis in Fig. 2B, fact that demonstrates the effective protection of PVA against oxidation.

DSC scans show the heat exchanged during sample heating and cooling over a defined temperature range. Fig. 5 reports the DSC curves of all the studied Mn samples: an endothermic irreversible event due to hydrogen desorption, with onset at about 150 °C and a peak temperature variable in the range 230–290 °C, is observed in all samples except the pristine Mn powder. This technique confirms the results of the diffraction experiments showing that even the slight oxidation of Mn produced by a short treatment in water is sufficient to partially hydrogenate the metal. In more extreme conditions (i.e. long oxidation or sonochemically-driven reactions) the amount of hydrogen

absorbed is greatly enhanced and a rich variety of behaviors is observed, which deserves further investigation.

3.2. Ultrasonic treatment of Ti microparticles

Titanium has been chosen because it forms a very stable hydride at ambient temperature and pressure and its formation is thermodynamically favored. Usually this material is synthesized using high pressure and high temperature conditions as the increase of temperature modifies the atomic cell from hcp to bcc, allowing the hydrogen enter more easily into interstitial sites of the metallic structure [7], [8]. We have performed several trials using simple aqueous suspension of Ti, and suspension of Ti in $NaBH_4$ solution, as in the case of Mn, but it was not possible to identify any Titanium hydride phase by XRD measurements. Indeed it is worth noting that, the hcp cell of Ti has octahedral sites quite large compared to the hydrogen radius, so the interstitial insertion of H atoms in hcp-Ti may not produce large effects on the cell size, making it harder to detect the formation of a Ti-H solid solution by XRD characterization. DSC measurements were then performed to spot any signal of hydrogen release upon heating, but their results were not conclusive: a very small endothermic signal was detected at low temperature (130 °C) only in samples treated in $NaBH_4$ solution, but a possible contamination of the sample with borate species with a certain amount of crystal water (borax, tincalconite), residue of the reaction solution, may also explain this small signal observed. It appears that, despite the thermodynamic stability, the hcp-cell and the presence of a very efficient passivating native oxide layer on the metal represent a limit for the formation of stoichiometric Titanium hydride by means of the sonochemical technique.

3.3. Ultrasonic treatment of $La(Fe,Si,Mn)_{13}$ intermetallic compound

The $La(Fe,Si,Mn)_{13}$ intermetallic compound is a magnetic phase which exhibits magnetocaloric effect, i.e. a temperature change due to the reversible magnetization and demagnetization process, driven by an applied field. This effect is related to the entropy change between the ferromagnetically ordered state and the paramagnetic disordered state. To exploit this temperature change in the cooling cycle of a refrigeration device, the ferromagnetic (FM) to paramagnetic (PM) transition temperature (Curie temperature) of the material has to be close to the operating temperature of the device (i.e. room temperature). Interestingly, the Curie temperature of the $La(Fe,Si,Mn)_{13}$ intermetallic can be modified by inserting interstitial hydrogen within the metal lattice, that forces the cubic cell to expand [33]. In particular, the transition temperature from the ferromagnetic to the paramagnetic state can be shifted around room temperature, making the hydrogenated compound $La(Fe,Si,Mn)_{13}H_x$ one of the most studied materials for magnetic refrigeration applications [34].

For this reason this magnetic compound has been used as a benchmark material to evaluate the effectiveness of the sonochemical (SC) process in comparison with the conventional hydrogenation technique, since its magnetic properties and thermal stability, which are strongly dependent on hydrogen content, are already known [34], [35]. Usually hydrogen adsorption of $La(Fe,Si,Mn)_{13}$ is performed in pure hydrogen atmosphere at high temperature (0.9–1 bar, 450–500 °C) [35]. As a starting material we used an intermetallic of nominal composition $LaFe_{11.47}Si_{1.28}Mn_{0.25}H_{1.65}$(for the sake of brevity called ‘Pristine compound’) which had been already hydrogenated by the

conventional process and we thermally treated it at 450 °C for 15 min, to promote hydrogen desorption (producing the ‘Dehydrogenated compound’), according to the reaction:

$La(Fe,Si,Mn)_{13}H_x + heat \rightarrow La(Fe,Si,Mn)_{13} + x/2H_2$

Then, the dehydrogenated compound was sonochemically treated to induce hydrogen uptake again. The ultrasonic treatment was performed in $NaBH_4$ solution, to prevent sample oxidation and to accelerate the rate of hydrogen absorption. As it shown in Fig. 6, through the XRD peak shape it was possible to follow the hydrogenation process of the $La(Fe,Si,Mn)_{13}$ compound performed by the sonochemical method. The process occurred in an incremental way after repeated treatments. The first treatment in $NaBH_4$ solution for 90 min produced a partial hydrogenation of the sample: a broad range of compositions was formed, with the tower-like XRD peak profile revealing an almost continuous increase of the lattice constant due to the incorporation of hydrogen into the intermetallic lattice. After 180 min of sonochemical treatment the compound was fully re-hydrogenated: its diffraction pattern and peak shapes were practically coincident with the ones of the pristine sample obtained through the gas-phase hydrogenation process, revealing that this technique can be used as a fast method to hydrogenate intermetallics too.

This is confirmed by the DSC curves shown in Fig. 7: the pristine compound shows two major endothermic events that are absent in the dehydrogenated compound: a small peak due to the reversible FM-PM transition and a huge peak due to the heat absorbed during hydrogen release from the metal lattice (irreversible process). The same features are observed in the sonochemically treated sample: the FM-PM transition in SC-treated sample is restored to the same temperature as in the original compound, an indirect evidence that the hydrogen content introduced into the metal lattice by ultrasonication is equivalent to the one of the conventional process; besides, a huge signal associated to hydrogen desorption is a further demonstration of the effectiveness of the sonochemical treatment. The onset of the hydrogen desorption process is shifted towards higher temperatures for SC-treated samples, a fact that deserves further investigations, since, contrary to the case of hydrogen storage materials, here the thermal stability of the hydrogenated compound is a beneficial property for its long-term application in magnetic refrigeration devices.

3.4. Possible mechanism of sonochemical hydrogenation

The results obtained with Mn microparticles evidenced that: i) spontaneous surface oxidation reactions in pure water supply enough hydrogen to promote a partial hydrogenation of the metal (interstitial solid solution) or even the formation of a 'high pressure' hydride with crystal structure different from the host metal; ii) hydrogen adsorption can be greatly accelerated by ultrasonic treatments. Usually hydride formation is described by the reaction:

$M + x/2H_2 \rightarrow MH_x$

in which M represent the generic metallic phase. To accomplish this, the H_2 molecule has to be dissociated leaving H radicals enter the structure as an interstitial atom. As a result, an α-hydride solid solution, containing hydrogen randomly distributed within the metal lattice, is formed. Interstitial hydrogen is responsible of the cell size expansion, as it was observed for both Mn and La-Fe-Si-Mn samples; then, after reaching a critical concentration, stoichiometric hydride formation occurs and new hydride phases are detected. To explain the acceleration of the process induced by

the sonochemical treatment we must consider that during sonication treatments several concurrent events are taking place. Firstly, the well known formation of H• and OH• radicals during sonication of water (water sonolysis) [36] can accelerate the hydride formation process, secondly, the high shear stress and mechanical forces on particles surfaces arising from bubbles oscillation and collapse, can increase the diffusion of hydrogen within the interstitial sites of the materials. Baidukova et al. [28] investigated the formation of Mg hydride particles under high intensity ultrasounds, observing that the formation of chemically modified nanostructured particles can be seen as a combination of these two effects. The results reported here show that the nature of the metal strongly influence this mechanism. Passivating properties, instability of the hydrides or thermodynamic barriers may hinder or prevent the hydrogenation as for the case of Ti particles that we have investigated. Additionally it should be considered that in common processes of gas-solid synthesis of hydrides (i.e. high pressure and high temperature) several steps which facilitate the introduction of hydrogen into the interstices can be accomplished at the same time, such as the structural phase transition to high temperature phase of the metal, and the thermal expansion of the metal lattice. Although the extreme conditions achieved by high intensity ultrasonic treatments, in some cases it was impossible to obtain pure metallic hydrides with this method. However the sonication of metallic particles in hydrogen-rich solutions opened new possibilities. By means of $NaBH_4$ hydrolysis the formation of hydrides and diffusion process within the metal can be accelerated and this could be beneficial for the case of intermetallics which may require the repetition of several cycles of hydrogen adsorption/desorption in conventional hydrogenation processes. During the sonication treatment hydrogen-rich bubbles nucleate in the bulk solution and on metal particles surfaces, increasing the amount of H [37] radical that can be injected within the particles by the mechanical effects of cavitation. The consequences of this mechanism have been clearly observed on both elemental metals and intermetallics from SEM characterization. In Fig. 8 the SEM pictures of the surface of coarse particles (~1 mm) of the $La(Fe,Si,Mn)_{13}$ compound before and after the sonochemical treatment are compared: although some hemispherical pores, formed during alloy solidification, are visible in the dehydrogenated sample (left), in the SC-treated sample (right) new morphological features are evident, i.e. small round craters that could be seen as the “trace” of the impact of collapsing bubbles on metallic surfaces.

Another synergistic effect of the ultrasonic treatment arises from the fact that, as the hydrolysis of $NaBH_4$ occurs, the increase of pH causes a decrease of the reaction rate reducing the H_2 gas formation, however the ultrasonic pulse induces the nucleation of hydrogen gas bubbles released into the solution acting as sort of accelerating tool of the reaction rate.

4. Conclusions and perspectives

The results obtained in this work show for the first time the possibility to use a simple ultrasonic set-up to synthesize metallic and intermetallic hydrides at room temperature and atmospheric pressure. The sonication of metallic and intermetallic particles slurries has been investigated both in pure water and in solution of a hydrogen-releasing reactant and the insertion of hydrogen atoms within the metal lattice, with formation of stable metal hydrides, has been demonstrated. The experimental conditions affecting the process have been investigated and optimized to obtain the sonochemical hydrogenation of an intermetallic compound whose magnetic properties (e.g. the FM-PM transition temperature) are well known and highly dependent on hydrogen content. The results reported here show as ultrasonic treatments can be used as a tool for top-down nanostructuring of

multiphase metal particles in order to obtain metal hydrides which commonly would require pure H_2 atmosphere with high pressures (~1 GPa). These experiments reveal as acoustic cavitation can be exploited as a cheap and fast synthetic method in fields still unexplored. As an example, preliminary results obtained on $LaNi_5$ (here not shown) indicate that this method could be promising also for hydrogen storage materials. Further investigation is needed to better understand the thermal behavior and stability of the hydride formed by this method and to compare it with the ones of the conventional hydrogenation process.

Acknowledgments

The authors wish to thank Vacuumschmelze GmbH for providing the La-Fe-Si-Mn-H samples. This work has been partially performed at NanoFacility Piemonte, an INRIM laboratory supported by Compagnia di San Paolo Foundation.

References

[1] N.A.A. Rusman, M. Dahari, A review on the current progress of metal hydrides material for solid-state hydrogen storage applications. Int. J. Hydrogen Energy, 41 (2016), pp. 12108-12126

[2] X. Yu, Z. Tang, D. Sun, L. Ouyang, M. Zhu, Recent advances and remaining challenges of nanostructured materials for hydrogen storage applications, Prog. Mater Sci., 88 (2017), pp. 1-48

[3] B.G. Pollet, The use of ultrasound for the fabrication of fuel cell materials, Int. J. Hydrogen Energy, 35 (2010), pp. 11986-12004

[4] Fu. Yuhao, *et al.*, High-pressure phase stability and superconductivity of pnictogen hydrides and chemical trends for compressed hydrides, Chem. Mater., 28 (2016), pp. 1746-1755

[5] M. Bououdina, *et al.*, Review on hydrogen absorbing materials—structure, microstructure, and thermodynamic properties, Int. J. Hydrogen Energy, 31 (2006), pp. 177-182

[6] A. Andreasen, Predicting Formation Enthalpies of Metal Hydrides, Risø National Laboratory (2004), pp. 1-33, ISSN 0106-2840 ISBN 87-550-3382-2

[7] H. Wipf, Solubility and diffusion of hydrogen in pure metals and alloys, Phys. Scr., 94 (2001), pp. 43-51

[8] V.E. Antonov, Phase transformations, crystal and magnetic structures of high-pressure hydrides of d-metals, J. Alloys Comp., 330–332 (2002), pp. 110-116

[9] J. Ren, N.M. Musyoka, H.W. Langmi, M. Mathe, S. Liao, Current research trends and perspectives on materials-based hydrogen storage solutions: a critical review, Int. J. Hydrogen Energy, 42 (2017), pp. 289-311

[10] M.V. Lototskyy, Metal hydride hydrogen compressors: a review, Int. J. Hydrogen Energy, 39 (2014), pp. 5818-5851

[11] E. Callini, *et al.*, Nanostructured materials for solid-state hydrogen storage: a review of the achievement of COST Action MP1103, Int. J. Hydrogen Energy, 41 (2016), pp. 14404-14428

[12] I. Lindemann, Synthesis of spherical nanocrystalline titanium hydride powder via calciothermic low temperature reduction, Scr. Mater., 130 (2017), pp. 256-259

[13] P. Hasina, Y. Wu, Sonochemical synthesis of copper hydride (CuH), Chem. Commun., 48 (2012), pp. 1302-1304

[14] K.S. Suslick, D.J. Flannigan, Ann. Rev. Phys. Chem., 59 (2008), pp. 659-683

[15] Sivakumar Manickam (Ed.), Cavitation A Novel Energy-Efficient Technique for the Generation of Nanomaterials, CRC Press Taylor & Francis Group, 6000 Broken Sound Parkway NW, FL 33487-2742 © (2014) by Taylor & Francis Group

[16] J.T. Han, Extremely efficient liquid exfoliation and dispersion of layered materials by unusual acoustic cavitation, Nature Sci. Rep., 4 (2014), p. 5133

[17] K.S. Suslick, Effects of high intensity ultrasound on inorganic solids, Ultrasonics, 25 (1987), pp. 56-59

[18] W. Zhang, W. He, X. Jing, Preparation of a stable graphene dispersion with high concentration by ultrasound, J. Phys. Chem. B, 114 (2010), pp. 10368-10373

[19] S.J. Chung, *et al.*, Characterization of ZnO nanoparticle suspension in water: effectiveness of ultrasonic dispersion, Powder Technol., 194 (2009), pp. 75-80

[20] D.G. Shchukin, *et al.*, Ultrasonic Cavitation at Solid Surfaces, Adv. Mater., 23 (2011), pp. 1922-1934

[21] E.V. Skorb, H. Möhwald, Ultrasonic approach for surface nanostructuring, Ultrason. Sonochem., 29 (2016), pp. 589-603

[22] E.V. Skorb, H. Möhwald, D.V. Andreeva, Effect of cavitation bubble collapse on the modification of solids: crystallization aspects, Langmuir, 32 (2016), pp. 11072-11085

[23] P.V. Cherepanov, D.V. Andreeva, Phase structuring in metal alloys: ultrasound-assisted top-down approach to engineering of nanostructured catalytic materials, Ultrason. Sonochem., 35 (2017), pp. 556-562

[24] J. Dulle, *et al.*, Sonochemical activation of Al/Ni hydrogenation catalyst, Adv. Funct. Mater., 22 (2012) (2012), pp. 3128-3135

[25] E.V. Skorb, D.V. Andreeva, H. Mohwald, Generation of a porous luminescent structure through ultrasonically induced pathways of silicon modification, Angew. Chem. Int. Ed., 51 (2012), pp. 5138-5142

[26] M. Virot, R. Pflieger, E.V. Skorb, J. Ravaux, T. Zemb, H. Mohwald, Crystalline silicon under acoustic cavitation: from mechanoluminescence to amorphization, J. Phys. Chem. C, 116 (2012), pp. 15493-15499

[27] A. Troia, A. Giovannozzi, G. Amato, Preparation of tunable silicon q-dots through ultrasound, Ultrason. Sonochem., 16 (2009), pp. 448-451

[28] O. Baidukova, *et al.,* Sonogenerated metal-hydrogen sponges for reactive hard templating, Chem. Commun., 51 (2015), pp. 7606-7609

[29] A. Mentler, *et al.,* Calibration of ultrasonic power output in water, ethanol and sodium polytungstate, Int. Agrophys., 31 (2017), pp. 583-588

[30] M. Pourbaix, Corrosion and metal artifacts – a dialogue between conservators and archaeologists and corrosion scientists, B. Floyd Brown, Harry C. Burnett, W. Thomas Chase, J. Goodway, M. Pourbaix Kruger (Eds.), Electrochemical Corrosion and Reduction, NBS Special Publication (1977)

[31] V.E. Antonov, T.E. Antonova, N.A. Chirin, E.G. Ponyatovsky, M. Baier, F.E. Wagner, T-P phase diagram of the Mn-H system at pressures to 4.4 GPa and temperatures to 1000°C, Scripta Mater., 34 (1996), pp. 1331-1336

[32] H.I. Schlesinger, H.C. Brown, A.E. Finholt, J.R. Gilbreath, H.R. Hoekstra, E.K. Hyde, Sodium borohydride, its hydrolysis and its use as a reducing agent and in the generation of hydrogen, J. Am. Chem. Soc., 75 (1953), pp. 215-219

[33] A. Fujita, S. Fujieda, Y. Hasegawa, K. Fukamichi, Itinerant-electron metamagnetic transition and large magnetocaloric effects in $La(Fe_xSi_{1-x})_{13}$ compounds and their hydrides, Phys. Rev. B, 67 (2003), Article 104416

[34] V. Basso, M. Küpferling, C. Curcio, C. Bennati, A. Barzca, M. Katter, M. Bratko, E. Lovell, J. Turcaud, L.F. Cohen, Specific heat and entropy change at the first order phase transition of La(Fe-Mn-Si)13-H compounds, J. Appl. Phys., 118 (2015), Article 053907

[35] A. Barcza, M. Katter, V. Zellmann, S. Russek, S. Jacobs, C. Zimm, Stability and magnetocaloric properties of sintered La(Fe, Mn, Si) H alloys, IEEE Trans. Magn., 47 (2011), p. 3391

[36] S.I. Nikitenko, R. Pflieger, Toward a new paradigm for sonochemistry: short review on nonequilibrium plasma observations by means of MBSL spectroscopy in aqueous solutions, Ultrason. Sonochem., 35 (2017), pp. 623-630

[37] M. Kohno, T. Mokudai, T. Ozawa, Y. Niwano, Free Radical formation from sonolysis of water in the presence of different gases, J. Clin. Biochem. Nutr., 49 (2011), pp. 96-101

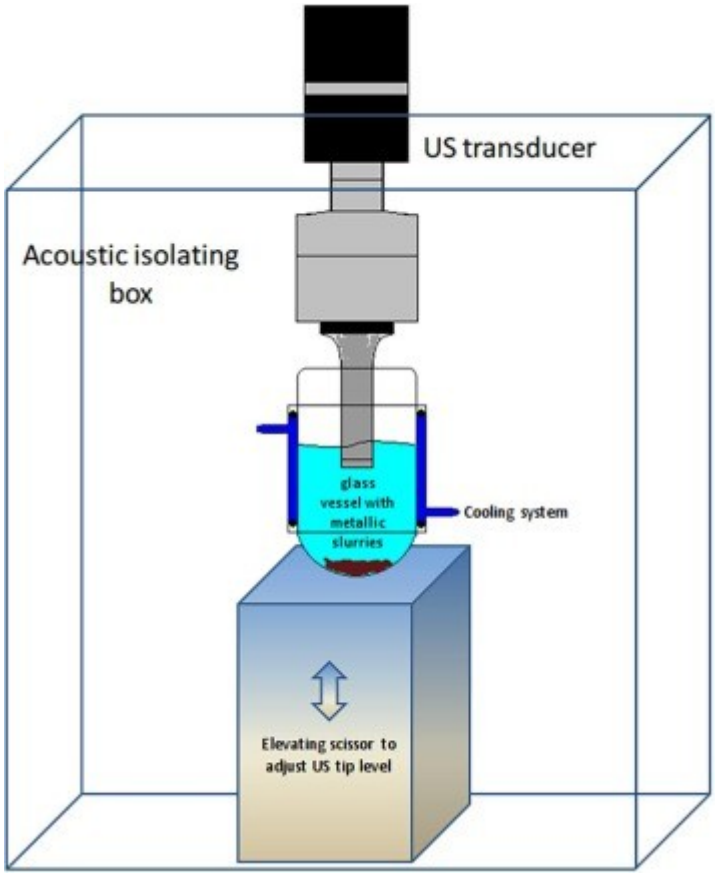

Fig. 1. Scheme of the experimental set up used for ultrasonic treatment of metallic microparticles.

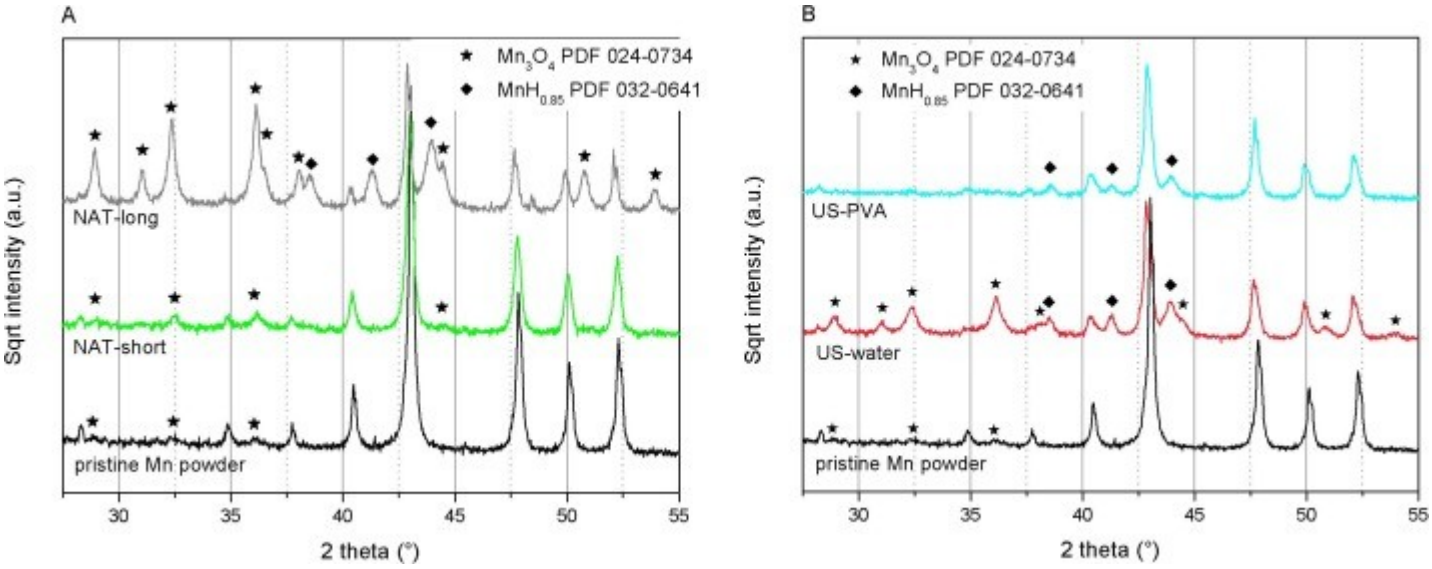

Fig. 2. X-ray diffraction patterns of selected Mn samples treated in deionized water: panel A) Natural oxidation condition: the sample was suspended in water for a short period (90 min, ID: NAT-short) or a longer one (1 month, ID: NAT-long); panel B) Sonochemical treatment in water: samples irradiated in US with and without PVA are compared. The pattern of the untreated Mn starting powder is also shown in both plots for comparison. Symbols identify the phases corresponding to the Powder Diffraction File (PDF) quoted in the legend. Peaks without symbols correspond to α-Mn(H).

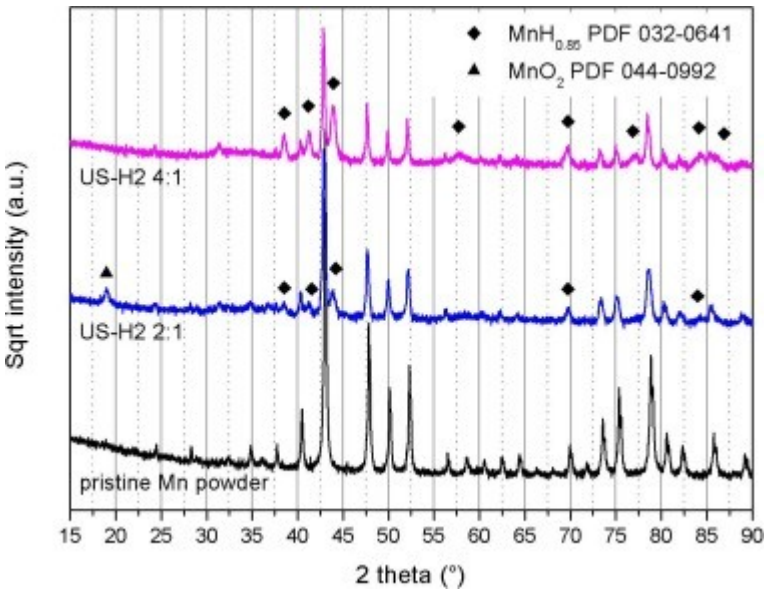

Fig. 3. X-ray diffraction patterns of selected Mn samples treated in $NaBH_4$ solution. Symbols identify the phases corresponding to the Powder Diffraction File (PDF) quoted in the legend. Peaks without symbols correspond to α-Mn(H).

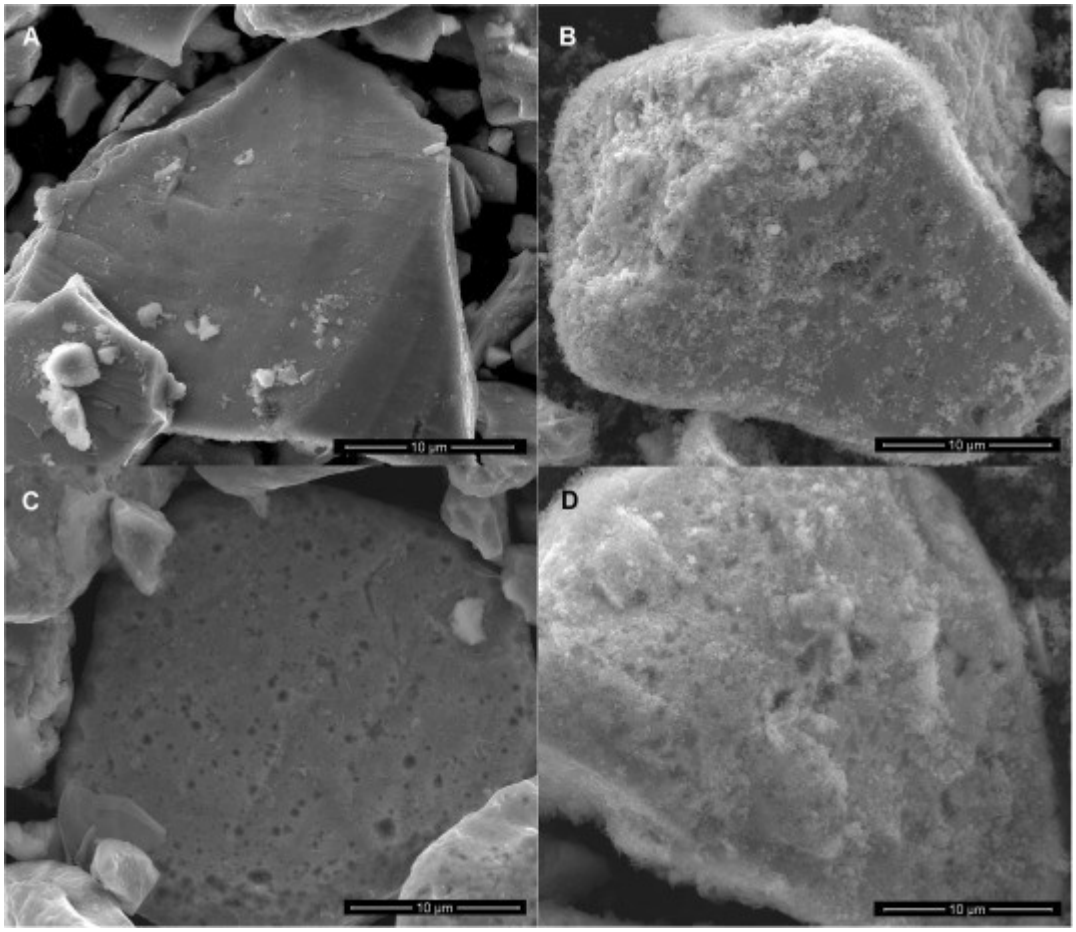

Fig. 4. SEM images of selected Mn samples: pristine powder (A), US-water sample (B), US-PVA sample (C) and US-H2 4:1 sample (D). See Table I for details on samples' treatment and phase composition.

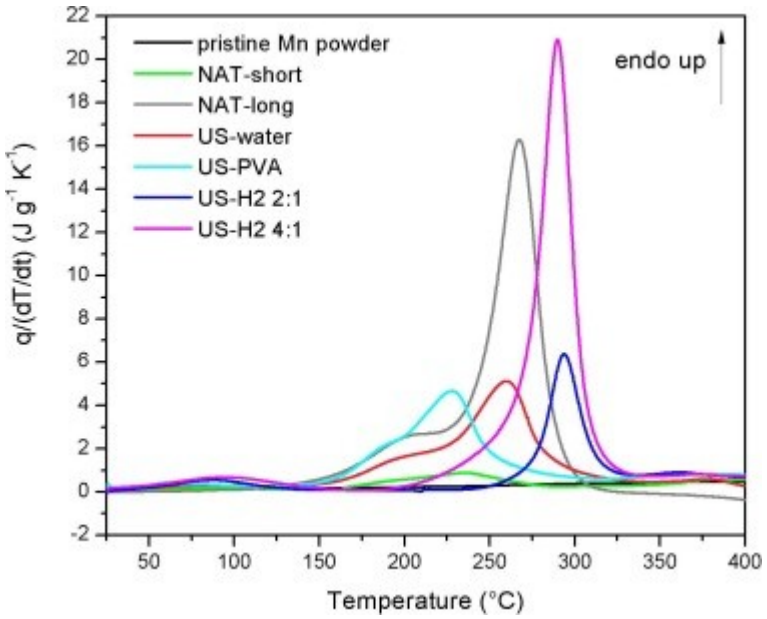

Fig. 5. DSC scans of the Mn samples (see samples ID in Table I). Each curve is obtained by subtraction of the signal of the second heating run from the first heating run performed on the same sample. Endothermic signals are reported as positive peaks.

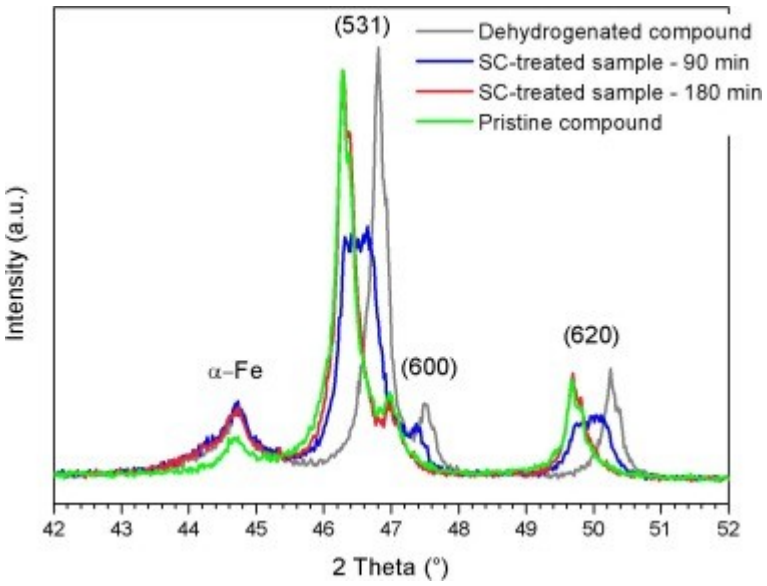

Fig. 6. X-ray diffraction patterns of the La(Fe,Si,Mn)$_{13}$ samples, before (dehydrogenated compound) and after (SC-treated samples) sonochemical treatments of different duration. The XRD pattern of the pristine compound (the starting powder prior to hydrogen desorption by thermal annealing) is also reported for comparison. A small angular range is considered to better display the peaks shift. Indexed peaks correspond to the cubic La(Fe,Si,Mn)$_{13}$(H) phase.

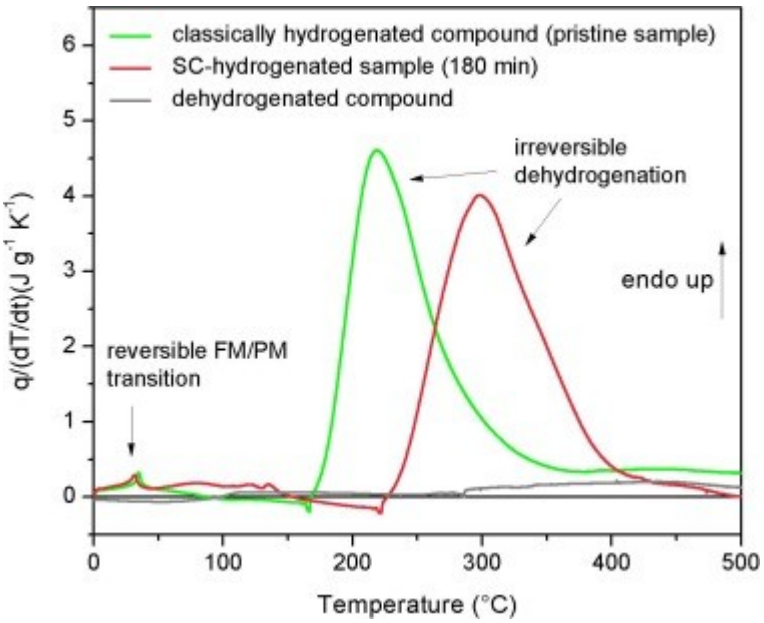

Fig. 7. DSC scans of the classically hydrogenated sample (pristine compound) and of the sonochemically (SC) hydrogenated sample. The scan of the dehydrogenated compound, showing no relevant features, is also reported for comparison. All the curves are obtained by subtraction of the signal of the second heating run from the first heating run performed on the same sample. Endothermic signals are reported as positive peaks.

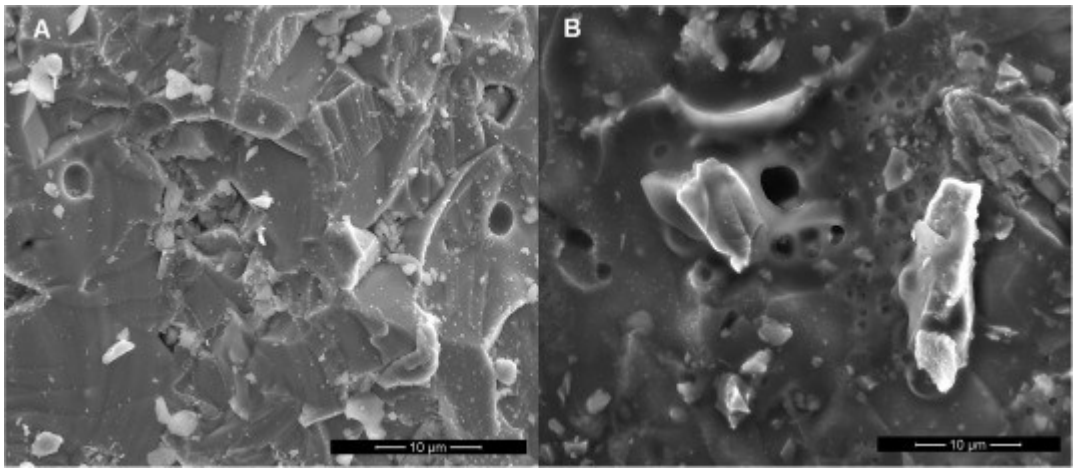

Fig. 8. SEM images of the surface of coarse particles (~1 mm) of the $La(Fe,Si,Mn)_{13}$ compound: A) dehydrogenated compound before the sonochemical treatment; B) sonochemically treated sample with the characteristic traces of microcavities induced by bubbles formation/collapse.